Est. 1984

ORIENTAL JOURNAL OF CHEMISTRY
An International Open Free Access, Peer Reviewed Research Journal

www.orientjchem.org

ISSN: 0970-020 X
CODEN: OJCHEG
2015, Vol. 31, No. (2):
Pg. 1185-1189

Polyaniline/$MnTiO_3$Nanocomposites: Fabrication, Characterization and Optical band gap

KHANAHMADZADEH SALAH[1]*, ENHESSARI MORTEZA[2], AMNIYATTALAB YASAMAN[1] and DAGHAYESH ROYA[1]

[1]Department of Chemistry, Mahabad Branch, Islamic Azad University, PO Box,443, Mahabad, Iran.
[2]Department of Chemistry, Naragh Branch, Islamic Azad University, Naragh, Iran.
*Corresponding author E-mail: khanahmadzadeh@iau-mahabad.ac.ir, khanamad_s@yahoo.com.

http://dx.doi.org/10.13005/ojc/310274

(Received: December 01, 2014; Accepted: January 12, 2015)

ABSTRACT

Polyaniline-manganesetitanate nano composites (NCs) with two contents loading of $MnTiO_3$ were successfully synthesized via sol–gel process using Manganese acetyl acetonate, tetra-n-butyltitanate, stearic acid, potassium iodate and sulfuric acid. The prepared PANI/MnTiO3NCs were characterized by energy dispersive X-ray spectroscopy (EDX), scanning electron microscopy (SEM), UV-vis diffused reflectance spectra (DRS), Particle Size Distribution (PSD)and Zeta Potential. The results indicated that $MnTiO_3$NPs with particle size between 22 and 30nm were distributed in PANI matrix. The value of direct band gap for $MnTiO_3$ and the PANI/$MnTiO_3$NCs with 10 and 20wt% of $MnTiO_3$NPs loading using the Tauc model came out to be 1.15 Ev, 1.35 and 1.25. Band gap analysis indicates semiconducting behavior of the NCs.

Keywords : nanocomposite,$MnTiO_3$, Zeta Potential, EDX, PSD, DRS

INTRODUCTION

PANI as a typical conducting polymer has recently received a great deal of attention. PANI is one of the most promising electrically conducting polymers due to its unique electrical and electrochemical properties, easy polymerization, high environmental stability and low cost of monomer[1-3],and its wide applications in microelectronic devices, diodes, light weight batteries, sensors, super capacitors, microwave absorption, corrosion inhibition[4-8], etc.The properties of PANI can be tailored by changing its oxidation states, dopants or through blending it with other organic, polymeric or inorganic nanosizedsemiconductingparticles.To obtain materialswith synergetic advantage between PANI and inorganic NPs, various composites of PANI with inorganic NPs such as CeO_2, TiO_2, ZrO_2, Fe_2O_3, and Fe_3O_4 are reported.The titanium-based oxides, such as barium titanate [9], cadmium titanate [10], bismuthtitanate [11], cobalt titanate [12] and lead titanate

[13], can be referred to as a'smart'familyowing to their excellent dielectric, piezoelectric, pyroelectric and photostrictiveproperties.Manganese ion in oxides is a well-known activator used mainly for producing tunablesolid-state laser media, holographic recording and optical data storage as well as thermoluminescentdetectors [14–16].Recently, manganese titanate ($MnTiO_3$) has attracted muchattention for its strong absorption in the visible region which may be propitious to theutilisation of solar energy [17] and photocatalysis [18].Manganese titanate, pyrophanite $MnTiO_3$, is a humidity sensing material withexcellent sensitivity, good selectivity, low temperature coefficient near zero and goodstability.The pyrophanite $MnTiO_3$ has also been studied for magnetic and photoelectro chemical properties [19–21].Physical properties (mechanical, thermal, etc.) of polymers can be improved by adding inorganic materials to polymer matrixes. In this study, PANI/$MnTiO_3$NCs with two (10, 20wt%) contents loading of $MnTiO_3$were prepared,andthe whole procedureand structural characterization of PANI/$MnTiO_3$NCs phases have been investigated by SEM, EDX, DRS, and Zeta Potential.

MATERIALS AND METHODS

Manganeseacetylacetonate, tetra-n-butyltitanate, stearic acid, potassiumiodate and sulfuric acid used in experimentswere all of analytical grade reagents.The composition of the sample was estimated using a model Oxford of Energy dispersive analysis of X-rays (EDX).The UV-vis diffused reflectance spectra (DRS) were obtained from UV-visScincom 4100 spectrometer. The SEM pictures were recorded withKYKYModelEM 3200instrument at the accelerating voltage of 25kV. Streaming zeta potential measurements were carried outon a ZetaCAD instrument (France).

Synthesis of $MnTiO_3$ nanoparticles

PANI/$MnTiO_3$composites were prepared along a synthetic procedure. $MnTiO_3$NPs were prepared through a modifiedwet-chemistry synthesismethod which is described in the literature[22]. In this procedure, a fixed amount of manganeseacetylacetonatewas added to the melted stearic acid and dissolved. Then, stoichiometric tetra-n-butyltitanate was added to the solution, stirred to form sol, naturally cooled down to room temperature, and was dried to obtain dried gel. Finally, the gel was calcined at 900°C in air to obtain $MnTiO_3$NPs.

Synthesis of PANI/$MnTiO_3$nanocomposite

In order to prepare ofPANI/$MnTiO_3$NCs,the essential substancesforpreparation of PANI were initiallyadded.TopreparePANI, 1g potassium iodate was added to 100 mlof sulfuric acid (1 M) and then uniform solution was resulted by using magnetic mixer. After 30 min, the sufficient amount of ultrasonicated $MnTiO_3$NPswas added to solution to prepare10 and 20 persent ofPANI/ $MnTiO_3$NCsand after 20min, 1 ml fresh distilledaniline monomer was added to stirred aqueous solution. The reaction was carried out for 5h at room temperature. Then the obtained product was dried at temperature about 60°C in oven for 24h[23].Finally after heat-treatment from 60°C to 300°C for 2h, the PANI/$MnTiO_3$NCs were obtained.The whole procedureand structural characterization of PANI/$MnTiO_3$NCs phases have been investigated by SEM, EDX, PSD, DRS, and Zeta Potential.

RESULTS AND DISCUSSION

DRS study

The absorption coefficient and optical band gap of a material are two important parameters bywhich the optical characteristics and its practical applications in various fields are judged.Fig.1. shows the DRS patterns of pure $MnTiO_3$ and the PANI/$MnTiO_3$NCs with 10 and 20wt% of $MnTiO_3$NPs loading. In fig.1a. a sharp absorption peak is observed around325nm, which indicates the optical band gap attributed to the $O^{2-} \rightarrow Ti^{4+}$ þcharge-transferinteraction[17]. Also in the PANI/$MnTiO_3$NCs with 10 and 20wt% of $MnTiO_3$NPs loadinga sharp absorption peak are observed around 345 and 350nm. Fordirectband gap determination, plot of $(ah\upsilon)^2$ versus $h\upsilon$ is presented in Fig . 2. Band gap value was obtained by extrapolating the straight portion of the graph on $h\upsilon$axis at =0, as indicatedby the solid line in Fig.2.The value of direct band gap for $MnTiO_3$and the PANI/$MnTiO_3$NCs with 10 and 20wt% of $MnTiO_3$NPs loadingusing the Taucmodelcame out to be 1.15 Ev, 1.35 and 1.25. Band gap analysis indicates semiconducting behavior of the NCs.

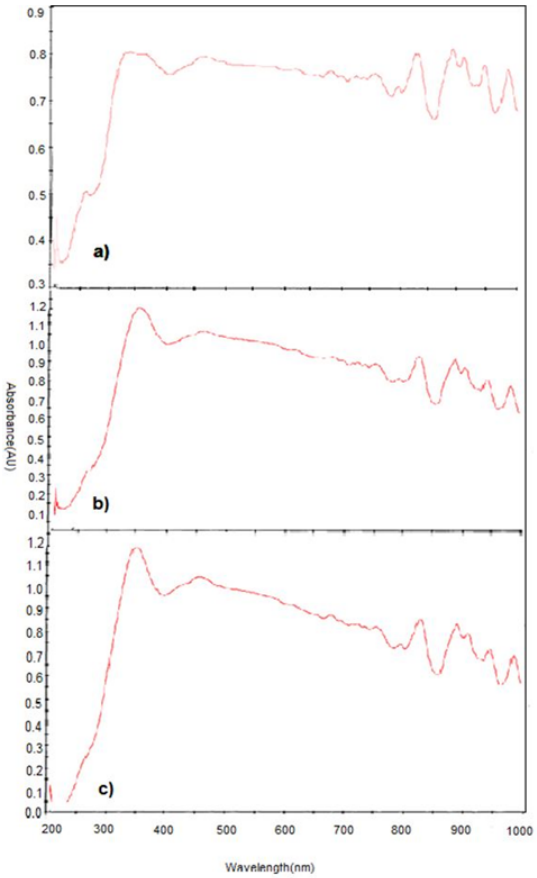

Fig. 1: DRS patterns of (a) $MnTiO_3$ nanopowders (b) PANI/ $MnTiO_3$ nanocomposite with $MnTiO_3$ content of (10 wt%) and (c) (20 wt%)

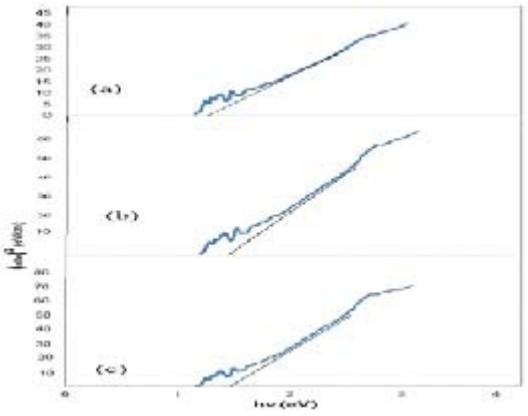

Fig. 2: Band gap patterns of (a) $MnTiO_3$ nanopowders (b) PANI/ $MnTiO_3$ nanocomposite with $MnTiO_3$ content of (10 wt%) and (c) (20 wt%)

Morphology of samples

Fig.3. shows the scanning electron micrograph of pure $MnTiO_3$ (Fig.3a.)) and the PANI/ $MnTiO_3$NCs with 10 and 20wt% of $MnTiO_3$NPsloading, respectively (Fig.3(b–c).). The particles have agglomerated graining structure.In the scanning electron micrograph of the NCs, with the increase of $MnTiO_3$content, the agglomeration become more appreciable and display some connections in some regions. SEM images reveal a homogeneous dispersion of $MnTiO_3$NPs in the PANI matrix.EDX patterns of pure $MnTiO_3$ (Fig.4(a).) and the PANI/$MnTiO_3$NCs with 10 and 20wt% of $MnTiO_3$NPs loading, respectively areshown in Fig. 4b. EDX patterns of pure $MnTiO_3$ (Fig .4(a).)shows

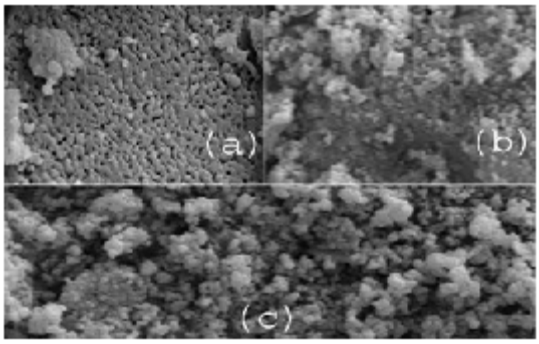

Fig. 3: SEM images of (a) $MnTiO_3$ nanopowders (b) PANI/ $MnTiO_3$ nanocomposite with $MnTiO_3$ content of (10 wt%) and (c) (20 wt%)

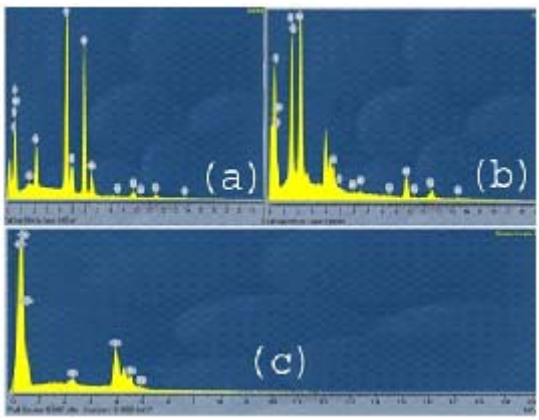

Fig. 4: EDX patterns of (a) $MnTiO_3$ nanopowders (b) PANI/ $MnTiO_3$ nanocomposite with $MnTiO_3$ content of (10 wt%) and (c) (20 wt%)

separate peaks of Manganese(Mn), Titanium (Ti), and Oxygen, which compositional analysis by EDX confirms that the $MnTiO_3$nanopowders were obtained. EDX pattern of PANI/$MnTiO_3$NCs with 10 and 20wt% of $MnTiO_3$NPs loading,are displayed in Fig.4b. which shows separate peaks of Manganese(Mn), Titanium (Ti), Oxygen, Carbon and Nitrogen (N), confirm that the sample is of desired composition having both the PANI and $MnTiO_3$ nanoparticles. The results show that as the $MnTiO_3$content increases in 10 and 20 weight fractions, the intensity of $MnTiO_3$ crystalline peaks gradually increases.

Particle Size Distribution (PSD)

Particle size distribution analysis (PSD) is a measurement designed to determine information about the size and range of a set of particles in a representative material. Particle size was determined using dynamic light scattering measurements. Fig.5. shows the size distribution histogram of pure $MnTiO_3$. The Zetasizer software uses algorithms to extract the decay rates for a number of size classes to produce a size distribution. The X-axis shows a distribution of size classes, whereas the Y-axis shows the relative intensity of the scattered light. The particle size distribution of the pure $MnTiO_3$ had a wide distribution (three peaks); therefore, its distribution is very heterogeneous. The particle size distribution of$MnTiO_3$for 88.2% of the particles were 85 nm, 6.4% were 250nm, and 5.4% were 1088 nm.

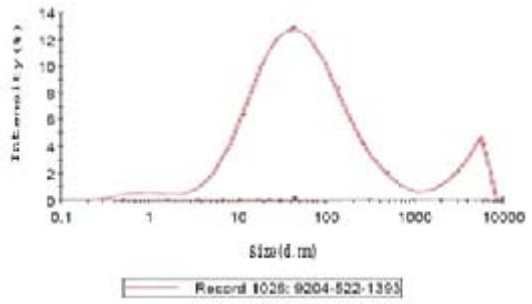

Fig. 5: PSD curves of $MnTiO_3$

Zeta potential measurements

Fig.6. shows the zeta potential measurements obtainedfor pure $MnTiO_3$ (Fig.6(a).) and the PANI/ $MnTiO_3$NCs with 10 and 20wt% of $MnTiO_3$NPs loading**.** Initially, $MnTiO_3$ had an average ζ of -9.75mV and the PANI/ $MnTiO_3$NCs with 10 and 20wt% of $MnTiO_3$NPs loading had an average ζ of -20 and -50.81 mV. With respect to Fig. 6.Zeta potential indicated that the fabricated PANI/$MnTiO_3$NCs with 10 and 20wt% of $MnTiO_3$NPs were increased with 34 and 67% efficiency respectively.

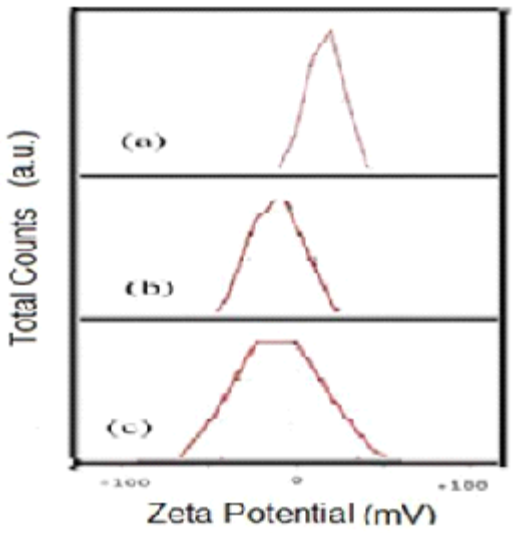

Fig. 6: Zeta potential patterns of (a) $MnTiO_3$ nanopowders (b) PANI/ $MnTiO_3$ nanocomposite with $MnTiO_3$ content of (10 wt%) and (c) (20 wt%)

CONCLUSION

We have successfully synthesized PANI/ $MnTiO_3$NCs with two (10, 20wt%) contents loading of $MnTiO_3$using wet chemical method. The whole procedure and structural characterization of PANI/ $MnTiO_3$NCs phases have been investigated by SEM, EDX, DRS, and Zeta Potential.The particle size distribution of $MnTiO_3$ for 88.2% of the particles were 85 nm, 6.4% were 250nm, and 5.4% were 1088 nm. Zeta potential indicated that the fabricated PANI/$MnTiO_3$NCs with 10 and 20wt% of $MnTiO_3$NPs were increased with 34 and 67% efficiency respectively.

ACKNOWLEDGEMENTS

The authors express gratitude and thanks to Islamic Azad University and the Iranian Nanotechnology Initiative for supporting this study.

REFERENCES

1. Majid, K.; Awasthi, S.; Singla, M.L. *J. Sensor Actuators A*. **2007**, *135*, 113-118.
2. Ansari, R.;Keivani, M.B. *E-J. Chem*. **2006**, *3*, 202-217.
3. Jiang, J.; Ai, L.;Li, L.-C. *J. Mater. Sci*. **2009**, *44*, 1024-1028.
4. Nandi, M.; Gangopadhaya, R.;Bhaumik, A. *Micropor. Mesopor. Mater*. **2008,** *109*, 239-247.
5. Zhao, C.; Xing, S.; Yu, Y.; Zhang, W.; Wang, C. *Microelectron. J.***2007**,*38*, 316-320.
6. Dalas, E.; Vitoratos, E.; Sakkopoulos, S.; Malkaj, P. *J. Power Sources*. **2004**, *128*, 319-325.
7. Ryu, K.S.; Lee, Y.; Han, K.S.; Park, Y.J.; Kang, M.G.; Park, N.G.; Chang, S.H.*Solid State Ionics*. **2004**, *175*, 765-768.
8. Manigandan, S.; Jain, A.; Majumder, S.; Ganguly, S.; Kargupta, K.*Sensor Actuators B*. **2008**,*133*, 187-194.
9. Xu,H.;Gao,L. *Mater. Lett.***2002**,*57*, 490–494.
10. Wang, H.;Zhang,X.;Huang,A.; Xu,H.; Zhu, M.; Wang, B.;Yan,H.; Yoshimura,M. *J. Cryst. Growth*. **2002**, *246*, 150–154.
11. Madeswaran,S.;Giridharan, N.V.;Jayavel,R. *Mater. Chem. Phys*. **2003**, *80*, 23–28.
12. Enhessari, M.; Parviz, A.; Ozaee, K.; Karamali, E. *J. Exp. Nanosci*. **2010**, *5(1)*,61–68.
13. Ohno, T.; Fu, D.; Suzuki, H.; Miyazaki, H.; Ishikawa, K. *J. Eur. Ceram. Soc*. **2004**, *24*, 1669–1672.
14. Gavrilovic,P.;Singh,S. *US patent No*. **1994**, *5*, 280, 534.
15. Noginov, M. A.*J. Opt. Soc. Am. BOpt. Phys*.,**1999,***16(1)*,3–11.
16. Zhydachevskii, Y.; Suchocki, A.; Berkowski, M.; Zakharko,Y. *Radiat. Meas*. **2007,** *42(4–5)*, 625–627.
17. Zhou,G.W.;Kang,Y.S. *Mater. Sci. Eng.***2004,** *24*, 71–74.
18. Song,Z.Q.;Wang,S.B.;Yang, W.; Li, M.; Wang, H.; Yan, H. *Mater. Sci. Eng.,* B.**2004,** *113*, 121–124.
19. Stickler,J.J.; Kern,S.;Wold,A.;Heller,G.S. *Phys. Rev.***1967,***164*, 765–767.
20. Watanabe,H.;Yamauchi,H.;Takei,H. *J. Magn. Magn. Mater*. **1980**,*15–18*, 549–550.
21. de Haart,L.G.J.;de Vries,A.J.;Blasse,G. *Mater. Res. Bull*. **1984,***19*, 817–824.
22. Enhessaria, M.;Parviz, A.; Karamali, E.; Ozae, K.*J. Exp. Nanosci*. **2012,***7(3),* 327-335.
23. Mansour, M.S.; Ossman, M.E.;Farag, H.A. *Desalination*. **2011**, *272*, 301-305.